

Experimental Investigation of Convective Heat Transfer during Night Cooling with Different Ventilation Systems and Surface Emissivities

Le Dreau, Jerome; Heiselberg, Per; Jensen, Rasmus Lund

Published in:
Energy and Buildings

DOI (link to publication from Publisher):
[10.1016/j.enbuild.2013.02.021](https://doi.org/10.1016/j.enbuild.2013.02.021)

Publication date:
2013

Document Version
Early version, also known as pre-print

[Link to publication from Aalborg University](#)

Citation for published version (APA):

Le Dreau, J., Heiselberg, P., & Jensen, R. L. (2013). Experimental Investigation of Convective Heat Transfer during Night Cooling with Different Ventilation Systems and Surface Emissivities. *Energy and Buildings*, 61(June), 308-317. <https://doi.org/10.1016/j.enbuild.2013.02.021>

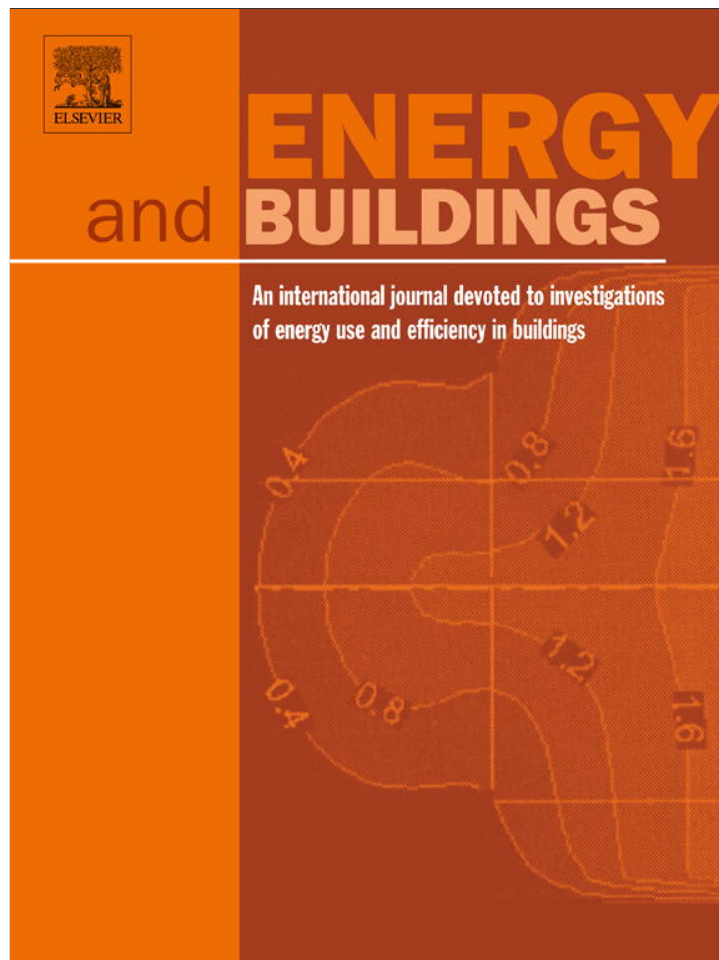
General rights

Copyright and moral rights for the publications made accessible in the public portal are retained by the authors and/or other copyright owners and it is a condition of accessing publications that users recognise and abide by the legal requirements associated with these rights.

- Users may download and print one copy of any publication from the public portal for the purpose of private study or research.
- You may not further distribute the material or use it for any profit-making activity or commercial gain
- You may freely distribute the URL identifying the publication in the public portal -

Take down policy

If you believe that this document breaches copyright please contact us at vbn@aub.aau.dk providing details, and we will remove access to the work immediately and investigate your claim.



This article appeared in a journal published by Elsevier. The attached copy is furnished to the author for internal non-commercial research and education use, including for instruction at the authors institution and sharing with colleagues.

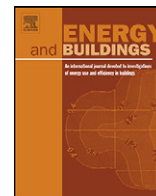
Other uses, including reproduction and distribution, or selling or licensing copies, or posting to personal, institutional or third party websites are prohibited.

In most cases authors are permitted to post their version of the article (e.g. in Word or Tex form) to their personal website or institutional repository. Authors requiring further information regarding Elsevier's archiving and manuscript policies are encouraged to visit:

<http://www.elsevier.com/authorsrights>

Contents lists available at [SciVerse ScienceDirect](#)

Energy and Buildings

journal homepage: www.elsevier.com/locate/enbuild

Experimental investigation of convective heat transfer during night cooling with different ventilation systems and surface emissivities

J. Le Dréau*, P. Heiselberg, R.L. Jensen

Department of Civil Engineering, Aalborg University, Sohngaardsholmsvej 57, DK-9000 Aalborg, Denmark

ARTICLE INFO

Article history:

Received 20 May 2012

Received in revised form 7 February 2013

Accepted 8 February 2013

Keywords:

Night-time ventilation

Full-scale experiments

Mixing ventilation

Displacement ventilation

Low-emissivity

Radiation pattern

Convective heat transfer coefficient

Mixed convection

Correlations

Local CHTC

ABSTRACT

Night-time ventilation is a promising approach to reduce the energy needed for cooling buildings without reducing thermal comfort. Nevertheless actual building simulation tools have showed their limits in predicting accurately the efficiency of night-time ventilation, mainly due to inappropriate models for convection. In a full-scale test room, the heat transfer was investigated during 12 h of discharge by night-time ventilation. A total of 34 experiments have been performed, with different ventilation types (mixing and displacement), air change rates, temperature differences between the inlet air and the room, and floor emissivities. This extensive experimental study enabled a detailed analysis of the convective and radiative flow at the different surfaces of the room. The experimentally derived convective heat transfer coefficients (CHTC) have been compared to existing correlations. For mixing ventilation, existing correlations did not predict accurately the convective heat transfer at the ceiling due to differences in the experimental conditions. But the use of local parameters of the air flow showed interesting results to obtain more adaptive CHTC correlations. For displacement ventilation, the convective heat transfer was well predicted by existing correlations. Nevertheless the change of floor emissivity influenced the CHTC at the surface of interest.

© 2013 Elsevier B.V. All rights reserved.

1. Introduction

One source of uncertainty in building simulation is the accurate simulation of convective heat transfer at the surface of the constructions. This uncertainty in the prediction is due to the complexity and diversity of flow that can be observed in buildings: the convective heat transfer can be either natural (driven by buoyancy forces), forced (caused by an external force) or mixed. As yearly simulations are required to analyze the building energy use, detailed analysis of the flow around and in the building is not possible and the calculation of convective heat transfer has to be simplified using correlations. Since the past 50 years, many researchers have studied experimentally convective heat transfer coefficients (CHTC) in order to improve the accuracy of simulations [1–9]. The first correlations were derived from flat plate experiments [1,2]. Nevertheless these correlations are not always applicable to buildings due to the scale effect and different flow characteristics: Awbi and Hatton [3] showed that the CHTC for a heated wall tends to be higher than that of isolated plates with free edges. Therefore full-scale measurements have also been performed under different conditions [3–9].

The most comprehensive model for CHTC available nowadays is probably the adaptive algorithm proposed by Beausoleil-Morrison [10], which consists in a coupling of different correlations. This model has been implemented in several Building Energy Simulation (BES) programs. Nevertheless high uncertainty can still be observed in the predicted energy consumption when forced convection is involved: some sensitivity analyses have showed that the predicted heating/cooling consumption could vary in the order of 20–40% depending on the model used for internal convection [10]. The interest of studying CHTC is therefore to improve the accuracy of BES tools.

Forced convection is the driving force of night-time ventilation. In many buildings, night-time ventilation is used instead of air conditioning to achieve thermal comfort during the summer season. The building structure is cooled down overnight with relatively cold outdoor air, in order to provide a heat sink during the occupied period of the next day by making use of the exposed thermal mass. Night-time ventilation showed a potential for energy savings, due to the time lag created between the occurrence of external and internal maximum temperatures [11]. Therefore it reduces the peak load of cooling demand, it makes possible the use of low grade cold source (i.e. outdoor air), and the operating cost can be decreased by making use of cheaper electricity during night-time. The interest for this concept has grown during the last few decades due to an increase of the cooling demand in buildings [12,13]. Artmann et al.

* Corresponding author. Tel.: +45 99408538.

E-mail addresses: jld@civil.aau.dk (J. Le Dréau), ph@civil.aau.dk (P. Heiselberg), rlj@civil.aau.dk (R.L. Jensen).

Nomenclature

A	surface area (m^2)
ACR	air change rate (/h)
Ar'	modified Archimedes number ($\text{K s}^2/\text{m}^6$)
CHTC	convective heat transfer coefficient
C_p	heat capacity (J/kg K)
D_h	hydraulic diameter of the entire surface (m)
E	energy (Wh/m^2)
ΔE_{i-j}	energy difference ($(E_i - E_j)/E_j$ (%)
E_b	black body emissive power (W/m^2)
F_{i-j}	view factor from surface i to surface j (–)
h	convective heat transfer coefficient ($\text{W/m}^2 \text{ K}$)
J	radiosity (W/m^2)
q	heat flux (W/m^2)
Q	heat flow (W)
T	temperature (K)
ΔT_{i-j}	temperature difference $T_i - T_j$ (K)
u	air velocity (m/s)
V_{flow}	flow rate at the inlet (m^3/s)
W	width of the nozzle opening (m)

Greek symbols

γ	convective ratio (–)
δ	Kronecker symbol (–)
ε	emissivity (–)
λ	thermal conductivity (W/m K)
ρ	density (kg/m^3)
σ	Stefan–Boltzmann constant ($5.6697 \times 10^{-8} \text{ W/m}^2 \text{ K}^4$)

Subscripts

cond	conduction
conv	convection
rad	radiation
tot	total
i or j	surface i or j

[14] have analyzed the climatic data in Europe and concluded that there is a high potential for night-time ventilation for the whole Northern Europe and a significant potential in Central, Eastern and even some regions of Southern Europe. But due to climate warming, the cooling potential might decrease and might be shifted from summer to transitions seasons [15].

Efficiency of night-time ventilation is highly dependent on the capacity of the building to absorb heat during day-time, but as well on its capacity to release the accumulated heat at night. During the design phase, engineers have therefore to make sure that the convective heat transfer is modelled accurately, in order to avoid overestimation of the capacity of night-time ventilation. Salmeron et al. [16] have analyzed numerically the capacity of night-time ventilation, and they found a variation by a factor 5 of the energy released depending only on the position of the inlet and outlet. Goethals et al. [11] showed that the choice of the convection algorithm is of the same importance as the design parameters. Using proper correlations should therefore be one of the main focuses when modelling night-time ventilation, especially because high air change rates are used.

In a previous study [17], Artmann et al. have investigated experimentally the efficiency of night-time ventilation with different types of ventilation. The results showed that displacement ventilation was more efficient than mixing ventilation for low air flow rates due to the large radiative exchange between the cold floor and the warm ceiling. A design chart was proposed to

estimate the global performance of night-time cooling. Artmann et al. investigated night-time ventilation as a system to cool down buildings, but were not focussed on characterizing CHTC in detail.

The purpose of this paper is to analyze the convective flow on the different room surfaces and compare with existing correlations. Most of these correlations have been derived from steady state experiments [1–9], only a few publications have derived CHTC from dynamic experiments [18,19]. Wallenten [18] analyzed CHTC for low air change rates and different configurations of heating. Goethals et al. [19] were focused on the impact of the room and system design on the efficiency of night-time ventilation; only the case of mixing ventilation at 8 ACH and a supply air temperature of 16.5°C was studied. It is therefore of interest to investigate the accuracy and the robustness of existing correlations in a dynamic case, with different air change rates, inlet air temperature and ventilation systems. Moreover an alternative way of deriving convective heat transfer coefficient will be attempted based on local data of the flow. This technique has first been used by Alamdari and Hammond [20] in 1987: they derived theoretically correlations for two and three-dimensional turbulent wall-jets based on basic flow theory. This method will only be applied to the surface directly affected by the inlet air, where there is a large convective exchange. Deriving the correlations from the flow characteristic could be a solution to improve their adaptability to the studied case, e.g. taking into consideration the type of inlet, the size of the room, the inlet temperature, etc.

Additionally the effect of a low-emissivity surface on the heat transfer has been analyzed by performing experiments with the floor covered by an aluminium foil. This type of coating is sometimes used in buildings to decrease the influence of one specific surface on the operative temperature. In Bangkok airport, a low-emissivity layer has been mounted at the ceiling, in order to decrease the influence of the warm ceiling on the radiant temperature, and therefore improving thermal comfort [21]. The other interest of having a low emissivity floor is to study the effect of a change in the radiation pattern on the heat that can be released from a thermal mass. During night-time ventilation, the thermal mass is releasing heat through convection and radiation to other surfaces, but this radiation pattern can change depending on the room layout (e.g. empty or a fully furnished room). These additional experiments will therefore emphasize the effect of the radiation pattern on the heat that can be released during night-time ventilation.

2. Experimental set-up

2.1. Test room

The experiments have been performed in the same test room than the one used by Artmann et al. [17] for investigating the efficiency of night-time ventilation. The test facility consists of an insulated wooden construction located in a laboratory at Aalborg University, Denmark. The internal dimensions of the test room are $2.64 \text{ m} \times 3.17 \text{ m} \times 2.93 \text{ m}$ (width \times length \times height) resulting in an internal volume of 24.5 m^3 . The thermal mass of the room is concentrated at the ceiling, which is composed of 7 layers of 12.5 mm gypsum boards. The other walls are highly insulated by 230 mm of expanded polystyrene (EPS). Considering daily variations of temperature, the dynamic thermal mass of the room is equal to $26 \text{ Wh/K m}^2_{\text{floor area}}$, which corresponds to a light building [22]. Compared to common buildings using night-time ventilation, the room has a lower thermal storage capacity, but the dynamic effects of night-time ventilation and the capacity of the ventilation system to discharge the thermal mass can still be observed.

Table 1
Properties of materials used in the test room.

Material	λ (W/m K)	ρ (kg/m ³)	C_p (J/kg K)	ε (–)
EPS	0.037 ± 0.001	16.0 ± 0.1	1450 ± 100	0.73 ± 0.05
Aluminium-foil (floor)	–	–	–	$0.03 - 0.004/+0.1$
Gypsum board	0.28 ± 0.01	1127 ± 10	1006 ± 100	–
White paint (ceiling)	–	–	–	0.9 ± 0.05

The thermal properties of the materials used in the test room and their associated uncertainties are described in Table 1. The properties used for calculation have been measured at EMPA (Swiss Federal Laboratories for Materials Science and Technology) or given by the manufacturer for the aluminium foil.

The test room is equipped with a mechanical ventilation system that supplies air at a defined temperature to the test room. The ventilation system consists of separate supply and exhaust systems. In order to obtain controlled conditions in the test room, the air supplied to the system is taken from the laboratory since the temperature in the laboratory is more stable than the outdoor air temperature. The ventilation system can provide from 56 m³/h up to 330 m³/h, corresponding to approximately 2.3–13.5 ACH. The set-up of the test room allowed choosing between two different types of ventilation, mixing or displacement ventilation. In case of mixing ventilation, the cold air is supplied directly below the ceiling, through a rectangular opening of 830 mm width and 80 mm height. The warm air is then exhausted close to the floor through two circular openings of 110 mm diameter. In case of displacement ventilation, the cold air is supplied through a semi-circular displacement device of 1015 mm height and 250 mm width, placed at the floor level in the middle of one of the short walls. The air is then exhausted through the rectangular opening located below the ceiling.

In order to establish the heat balance of the test room, the temperatures in the different construction parts are monitored at a frequency of 0.1 Hz. Each surface has been discretized in a finite number of sections, assuming that the temperatures measured by the thermocouples are representative of the whole section. The test room has been subdivided in a total of 37 sections. A high temperature gradient is expected to occur at the ceiling, especially in case of mixing ventilation; therefore the ceiling has been subdivided in 22 sections, with smaller sections close to the inlet in order to ensure a reasonable accuracy. At each of these 22 sections, 5 thermocouples are recording the temperature profile through the gypsum layers. As for the walls and the floor, they have been subdivided into 3 sections each. At each section, 1 thermocouple measures the surface temperature and 1 thermopile made of four junctions measures the temperature difference inside the construction, over a 30 mm layer of EPS (100–130 mm far from the surface). The air temperature is measured by three columns of thermocouples placed in the symmetrical axe of the test room. The thermocouples are placed 10 cm, 110 cm, 170 cm, 260 cm and 290 cm above the floor. Additional thermocouples are placed in the inlet and outlet of the ventilation system. All thermocouples used in these experiments are type K thermocouples and are connected to two Fluke Helios Plus 2287A data loggers.

2.2. Procedure for experiments

Before starting the experiments, the test-room temperature is stabilized at the laboratory temperature in order to ensure that the thermal mass is fully charged. Then cold air is supplied to the test room during 12 h under different conditions to simulate night-time ventilation. A total of 34 experiments have been performed, with different air change rates (2.3, 3.1, 6.7 and 13 ACH), different ventilation types (mixing and displacement), different types of

flooring (normal and low emissivity) and different inlet temperatures (ΔT_0 varying between 2.9 and 12.7 K, with ΔT_0 difference between the mean temperature at the ceiling before starting the experiment and the mean inlet temperature measured during the last 10 h of the experiment). A first set of experiments has been performed by Artmann et al. in 2008 with the floor made of EPS [17]. In 2009 similar experiments have been conducted using an aluminium floor cover, in order to observe the influence of different surface emissivity on the room heat flow. Displacement ventilation and mixing ventilation have also been used in that case. A detailed list of experiments can be found in [23,24].

3. Data analysis

3.1. Establishing the energy balance of the room

In order to calculate the heat removed by night-time ventilation, the energy balance of the test room has to be established. For each section, the conductive and radiative heat flows at the surfaces of the test room are calculated from the measured temperatures and material properties; the convective flow is then determined as the difference between conduction and radiation on each section.

A one-dimensional finite difference model with an explicit scheme has been used to determine the conductive heat flux at each section [25]. Each section has been discretized into a minimum of 20 finite elements. At the ceiling, the temperatures measured at the surface and 87.5 mm deep inside the construction are used as boundary conditions of the calculation. The accuracy of the calculation has been tested by comparing the calculated and the measured temperature profile. At the floor and at the walls, the temperature measured at the surface and the temperature difference measured 115 mm deep inside the construction are used as boundary conditions. This temperature difference is obtained over a 30 mm layer of EPS, and is then converted into a heat flux, assuming linear temperature profile between the thermopile; this assumption leads to a maximum error of 0.04 K between the measured temperature difference and the calculated one. In order to reduce the noise in the measurements, the moving average technique was used. The surface sensors are affected by radiation and convection, therefore a longer moving average has been applied on them: their signals have been averaged over 450 s (45 values), whereas the signals coming from sensors embedded in the constructions have been average over 100 s (10 values).

For the calculation of the radiative heat flow, different methods used nowadays in BES programs have been tested in order to study their influence on the room heat balance. The main difficulty for calculating radiation in an enclosure composed of diffuse grey surfaces arises from the treatment of the multiple reflections. Some of these techniques are based on the calculation of view factors F_{i-j} between the different sections; they have been determined according to [26]. The different models tested are the following:

Model 1: 2-surfaces forming an enclosure, infinite reflections [27]. This model, which is used in the program IES(VE), calculates the radiative exchange by merging the surrounding surfaces into one surface. This calculation method, also

known as the mean radiant temperature method, is rather simple: no view factors are used, only area weighted values are calculated.

$$q_{\text{radi}} = \frac{6}{5} \cdot \frac{5.7}{1 + (1 - \varepsilon_i)/\varepsilon_i + (A_i/\sum_{j \neq i} A_j)(1 - \varepsilon_{j \neq i})/\varepsilon_{j \neq i}} \cdot (T_i - \bar{T}) \quad (1)$$

$$\text{where } \bar{\varepsilon}_{j \neq i} = \frac{\sum_{j \neq i} A_j \varepsilon_j}{\sum_{j \neq i} A_j}$$

$$\bar{T} = \frac{\sum_j A_j T_j}{\sum_j A_j}$$

Model 2: 2-surfaces interaction, infinite reflections [28]. This equation has been used by Artmann et al. [17] in the previous analysis of the experiments. If the surface emissivities are around 0.8, this method accounts for about 81% of the energy emitted by the surfaces (cf. Clarke [29]).

$$q_{\text{radi}} = \sigma \sum_j \frac{\varepsilon_i \cdot \varepsilon_j \cdot F_{i-j}}{1 - (1 - \varepsilon_i)(1 - \varepsilon_j) \cdot F_{i-j} \cdot F_{j-i}} \cdot (T_i^4 - T_j^4) \quad (2)$$

Model 3: 2- and 3-surfaces interaction, infinite reflections [29]. With this equation, the flux going from surface i , reflected by a third surface and arriving to surface j is taken into consideration. According to Clarke [29], this method accounts for about 95% of the energy emitted by the surfaces for surface emissivities around 0.8. In case of low emissivity surfaces, the error will become larger, and more advanced models should be used. This calculation method has been implemented in ESP-r.

$$q_{\text{radi}} = \sigma \sum_j \left[\frac{\varepsilon_i \cdot \varepsilon_j \cdot F_{i-j}}{1 - (1 - \varepsilon_i)(1 - \varepsilon_j) \cdot F_{i-j} \cdot F_{j-i}} + \varepsilon_i \cdot \varepsilon_j \cdot A_j \cdot \sum_k \left(\frac{(1 - \varepsilon_k) \cdot F_{i-k} \cdot F_{j-k}}{A_k \cdot (1 - (1 - \varepsilon_i)(1 - \varepsilon_j)(1 - \varepsilon_k) \cdot F_{i-k} \cdot F_{k-j} \cdot F_{j-i})} \right) \right] \cdot (T_i^4 - T_j^4) \quad (3)$$

Model 4: n -surfaces interaction, infinite reflections (exact solution) [30]. The radiosity method is based on the construction of an equivalent network to represent the interaction between surfaces. This technique is used in EnergyPlus and IDA-ICE, and a similar method (named Gebhart factors) can be activated in TRNSys 17. For an enclosure, the following system has to be solved:

$$\left[\frac{\delta_{ij} - (1 - \varepsilon_i) \cdot F_{i-j}}{\varepsilon_i} \right] [J_i] = [E_{bi}] \quad (4)$$

$$q_{\text{radi}} = \frac{\varepsilon_i}{(1 - \varepsilon_i)} \cdot [E_{bi} - J_i]$$

Table 2 gives the resulting radiative heat flux at the ceiling obtained with the different models. Only one case is detailed, but similar behaviour can be observed with other experiments. When using model 2, the error on the calculated radiative heat flux is around 3 W/m². Models 1 and 3 have a better accuracy, with an error around 1 W/m²; nevertheless this level of accuracy is too low

Table 2

Mean radiative heat flux from the ceiling during the 3rd hour with different calculation methods for radiation. Experiment with mixing ventilation and aluminium flooring, 6.7 ACH and $\Delta T_0 = 9.4$ K.

	Model 1	Model 2	Model 3	Model 4
$Q_{\text{rad Ceiling}}$ (W/m ²)	9.8	5.7	7.8	8.7
$\Delta Q_{\text{Model 4}}$ (%)	12.3%	−34.8%	−10.5%	−

when considering the range of convective flow observed in the test-room. Therefore the radiosity method has been chosen to analyze the experimental results (the developed model has been verified against [30]).

3.2. Determination of the convective heat transfer coefficients

Convective heat transfer coefficients (CHTC) can be derived from the convective heat flux as follow: $q_{\text{conv}} = h \cdot \Delta T_{\text{Surface-Reference}}$. The value of h is therefore highly dependent on the reference temperature used ($T_{\text{Reference}}$) and will depend on the type of flow. CHTC used in building applications can be divided in three categories:

- *natural convection* is driven by buoyancy forces resulting from surface-to-air temperature differences. CHTC are usually expressed as a function of the temperature difference between the surface and the room air ($\Delta T_{\text{Surface-Room air}}$) and $q_{\text{conv}} = h_{\text{natural}} \cdot \Delta T_{\text{Surface-Room air}}$.
- *forced convection* is generally caused by an external force, i.e. a fan or the wind. CHTC are usually expressed as a function of the air change rate (ACR) and $q_{\text{conv}} = h_{\text{forced}} \cdot \Delta T_{\text{Surface-Inlet air}}$, with $\Delta T_{\text{Surface-Inlet air}}$ temperature difference between the surface and the inlet air.
- *mixed convection* occurs when both mechanical and buoyancy forces are important. One technique commonly used to derive CHTC in such a case is Churchill and Usagi method [31], which interpolates two independent variables between limiting solutions: $h_{\text{mixed}}^n = h_{\text{natural}}^n + h_{\text{forced}}^n$, with n blending coefficient. Different values have been chosen for n depending on the cases: Beausoleil-Morrison [32] and Novoselac [33] defined this blending coefficient to 3, whereas the value $n=3.2$ was used by Neiswanger et al. [34] and Awbi and Hatton [6]; Novoselac et al. [9] used $n=6$ for displacement ventilation because it showed better agreement with experimental results.

For more information, the reader can refer to the detailed literature review of existing correlations performed by Peeters et al. [35].

The experimentally derived CHTC will be analyzed for each surface, and compared with existing correlations. As the convective flow in the room is mainly driven by the inlet velocity, experimental data will be compared to forced correlations. Mixed correlations give similar results to that of forced correlations, and will therefore not be presented in the following parts. Temperature sensors are logged every 10 s, and then a moving average over 7.5 min is used to assess the surface temperatures; it has therefore been decided to evaluate the mean CHTC over a 30 min interval. The room air temperature is defined as the average values of 6 thermocouples located in the mid-section of the room, three at 1.1 m high and three others at 1.7 m high.

3.3. Uncertainty analysis

In order to evaluate the accuracy of the results, it is important to perform an uncertainty analysis taking into consideration the different experimental parameters. The uncertainty on the temperature measurements and on the construction parameters has

been evaluated, and the total uncertainty on the derived heat flux has then been calculated using the Monte Carlo analysis. For each experiment, 300 simulations have been performed with the randomly generated parameters. The resulting uncertainty is given with a confidence interval of 95%.

The accuracy of the temperature measurement system was estimated to be ± 0.086 K (confidence interval of 95%, normally distributed). This uncertainty takes into consideration the data logger resolution, the composition of thermocouples, the accuracy of the ice point reference and the calibration. Details can be found in the technical report from Artmann et al. [36]. At each section of the floor and the walls, one thermopile made of four junctions is recording the temperature difference: the uncertainty can therefore be decreased down to ± 0.058 K, to which is added 0.04 K for taking into consideration the linearization of the heat flux. When measuring temperature in a room, thermocouples can be affected by incoming radiation. Therefore an additional uncertainty is added to the surface thermocouples: ± 0.010 K/(W/m²) of radiative flux for the ceiling, and ± 0.042 K/(W/m²) for the other walls. These values have been calculated assuming that the emissivity of the measuring area was varying up to 0.15 and 0.4 respectively compared to the considered surface. At the ceiling the uncertainty is smaller as the sensors were mounted before the ceiling was painted. Finally the uncertainty on the air temperature is equal to 27% of the temperature difference between the surfaces and the measured room air. This value assumes that thermocouples have a surface emissivity of 0.2 and are subject to a natural convective flow.

The accuracy on construction materials is given in Table 1. The uncertainties are given with a confidence interval of 95% and are normally distributed, except for the emissivity of the aluminium flooring. In fact due to the effect of time, the emissivity of this product is expected to increase. Therefore a χ^2 -distribution (with 6 degrees of freedom) has been chosen, resulting in a non-centred distribution with a 95%-confidence interval of $[\varepsilon - 0.004; \varepsilon + 0.1]$. The left-hand side corresponds to the accuracy of the equipment used to measure emissivity. Accuracy on the construction thickness has also been taken into consideration [37].

4. Results for mixing ventilation

4.1. Mean convective flow and influence of the low-emissivity flooring

Fig. 1 represents the mean convective flux removed from the test room depending on the temperature difference between the average surface temperature of all surfaces (area weighted) and the inlet. The grey bands indicate the 95% uncertainty bands. The uncertainty on the convective heat flux is larger at the beginning of the experiments due to the large temperature variations. First of all, it can be observed that the convective flux decreases over the time, i.e. when the temperature difference between the surfaces and the inlet decreases. Moreover the convective flux increases when a higher air change rate is applied.

When comparing the total heat flux removed from the test room with and without aluminium flooring, almost no difference can be observed. For the same air change rate, the results of the two sets of experiments lie within the uncertainty bands. Only for 13 ACH a difference can be observed: the convective heat flow is lower with the aluminium flooring; but this difference can be explained by the slightly smaller air change rates in that case (around 0.3ACH smaller). These observations denote that decreasing the radiative flow at the floor does not influence the global room heat balance. Part of the heat initially released at the floor might be transferred to other surfaces: it is therefore of interest to compare the convective flow on individual surfaces with and without aluminium flooring.

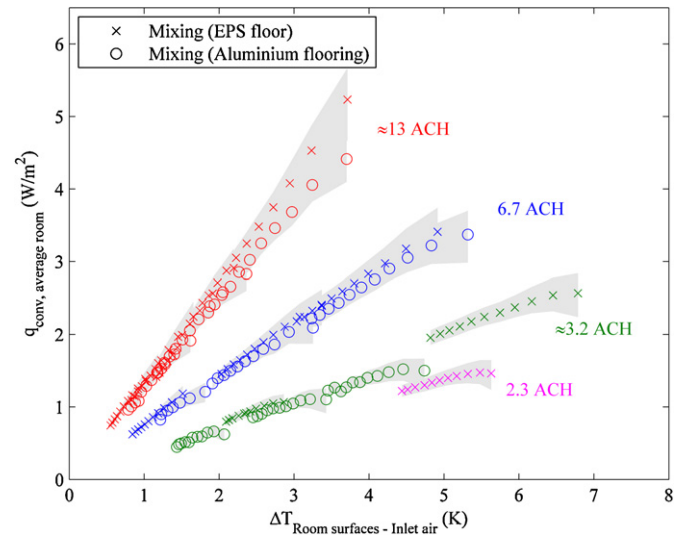


Fig. 1. Mean convective heat flux from all surfaces depending on the temperature difference between the mean surface temperature and the inlet air temperature – mixing ventilation.

In order to characterize the convective flow in the room as a function of the air flow pattern, a modified Archimedes number will be used. Artmann et al. [17] showed a linear relation between the ratio of convective to total heat flow from the ceiling depending on the Archimedes number: this parameter can therefore be used to compare the different experiments. The modified Archimedes number is defined as [17]:

$$Ar' = \frac{T_{surfaces} - T_{inlet}}{V_{flow}^2} \quad (5)$$

For each surface i , the convective ratio γ_i is calculated: $\gamma_i = Q_{conv,surface i} / Q_{conv,tot}$ with $\sum \gamma_i = 1$ for the entire room. Fig. 2 shows the distribution of the convective flow on the room surfaces. It can be observed that the convective flow from the ceiling is decreasing rapidly when the air change rate is decreasing: at small Archimedes numbers (lower than 100), 40% of the convective flow comes from the ceiling, whereas this value goes down to 5% when Archimedes number is equal to 10,000. At low air change rate, the jet is falling down right after the inlet due to its low momentum and the high temperature gradient between the ceiling and the inlet air. As the heat cannot be removed directly from the ceiling by convection, it is transferred to the surrounding surfaces by radiation. The view factors from the ceiling to the four walls and the floor are all equal to 0.2, resulting in a heat flow almost equally reported on these five surfaces.

When comparing the distribution of the convective flow on the room surfaces with and without the aluminium flooring, it can be observed that the convective flow at the floor is dropping when an aluminium foil is used because the heat exchange between the ceiling and the floor becomes extremely small. But this change of the room heat balance does not affect the part of convective flow extracted from the ceiling. The convective flow initially released at the floor is shared out among the walls.

4.2. CHTC at the ceiling

4.2.1. Comparison of flow and convective ratio

The velocity at 18 different positions of the ceiling has been measured for 8 experiments with the floor made of EPS. The anemometers were placed 30 mm below the ceiling and the velocity was measured for a time period of half an hour. In Fig. 3, the local dimensionless velocity at the ceiling (u/u_{inlet}) is compared to the

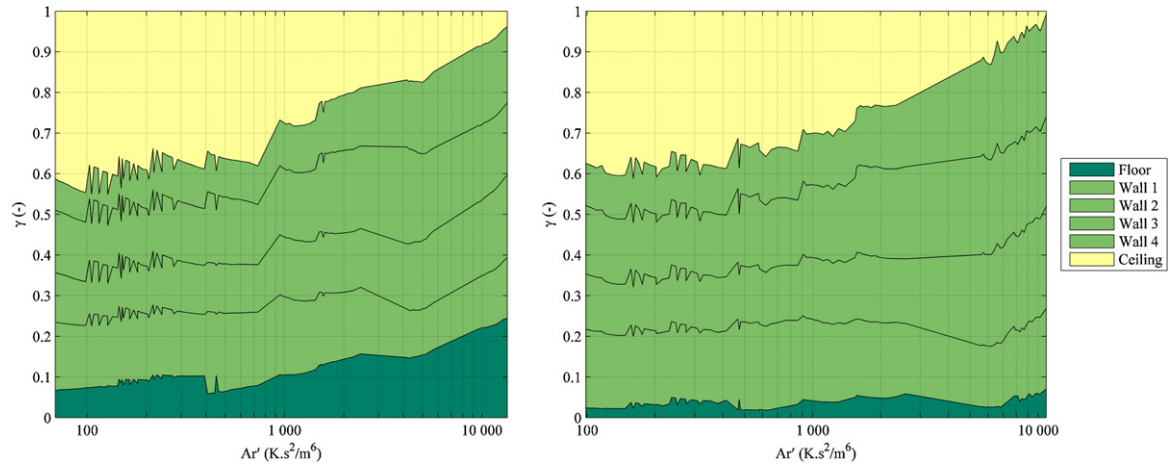


Fig. 2. Ratio of convective to total heat flow from the different surfaces depending on the Archimedes number (left: floor made of EPS – right: aluminium flooring) – mixing ventilation.

local convective ratio (γ_{local}), with $\gamma_{\text{local}} = Q_{\text{conv,section } i} / Q_{\text{cond,section } i}$. At low air change rate (3.2 ACH), it can be observed that the jet is falling down right after the inlet, resulting in a low convective ratio on the entire surface; the average Archimedes number is higher than 100, indicating the dominance of buoyant forces. Conversely the jet is covering a large part of the ceiling at high air change rate (13.2 ACH), resulting in a high convective ratio: the average Archimedes number is lower than 1, indicating the dominance of forced convection. Moreover it can be observed that there

is a strong relationship between the dimensionless velocity and the local convective ratio.

4.2.2. Average value over the ceiling

Fig. 4 compares experimental values of convective heat transfer coefficients to existing correlations: Fisher [7], Fisher and Pedersen [8] and Awbi and Hatton [6]. For the sake of clarity, uncertainties are not represented on the figure, but the average value is mentioned in the figure caption.

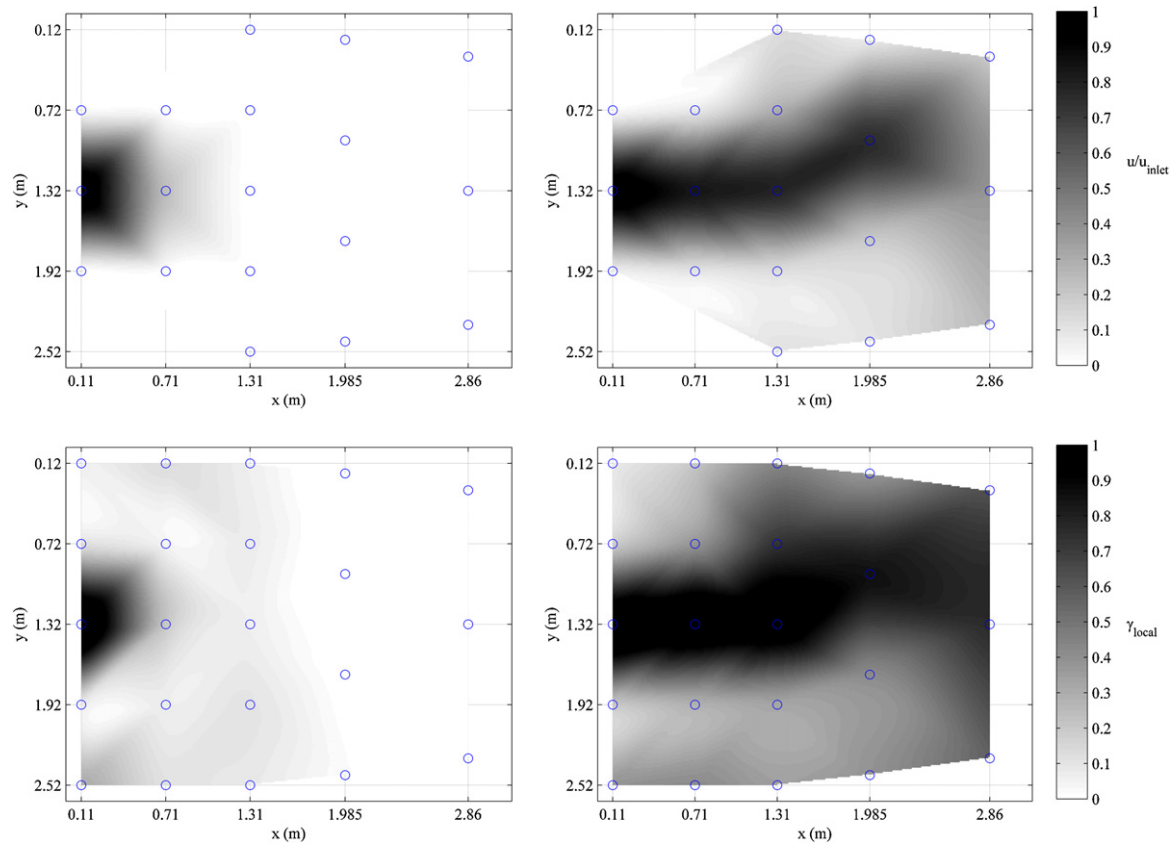


Fig. 3. Comparison of the local dimensionless velocity (upper graphs) and the local convective ratio (lower graphs) at the ceiling for 3.3 ACH (on the left) and 13.2 ACH (on the right).

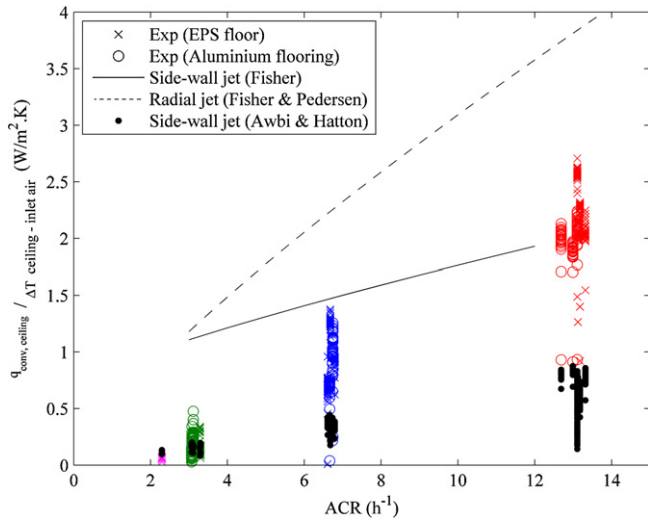


Fig. 4. CHTC at the ceiling depending on the air change rate. Mean uncertainty: (0.068 ACH) W/m² K.

Fisher [7] investigated the convective heat transfer coefficients in a test facility where cold air was supplied in the middle of a side-wall. The internal dimensions of the test room were 2.7 m × 4.6 m × 2.7 m (width × length × height) and the heat balance was performed dividing the test room into 53 sections. Due to the jet deflection, the largest CHTC has been observed at the floor and is equal to: $h = 0.704 + 0.168 \text{ACH}^{0.8}$, using the inlet air as reference temperature. Some discrepancies between this correlation and the experimental results can be expected as the two studied surfaces have different aspects. In the same test facility, Fisher and Pedersen [8] studied the convective flow with a radial ceiling diffuser, supplying cold air between 3 and 12 ACH. The CHTC for forced convection at the ceiling is equal to: $h = 0.49 \text{ACH}^{0.8}$, using the inlet air as reference temperature. Awbi and Hatton [6] also investigated the convective flow due to a cold jet over a heated ceiling. The air change rate varied between 1.2 up to 11.7 ACH. The internal dimensions of the test room were 2.8 m × 2.8 m × 2.3 m (width × length × height) and each surface was divided into 4 sections. The correlation resulting from this experiment is expressed as a function of the width of the nozzle opening W and the inlet velocity u_{inlet} : $h = 1.35W^{0.074}u_{\text{inlet}}^{0.772}$, using the local air as reference temperature (100 mm far from the surface). In order to use the same reference than Fisher, a factor ($\Delta T_{\text{Ceiling-Room air}} / \Delta T_{\text{Ceiling-Inlet air}}$) has been applied on this CHTC.

Measured CHTC are lower than the one proposed by Fisher and Pedersen [8]. In fact Fisher and Pedersen were using a radial ceiling diffuser, which is more efficient than a side-wall diffuser because the air jet is covering a larger area. When comparing to the results

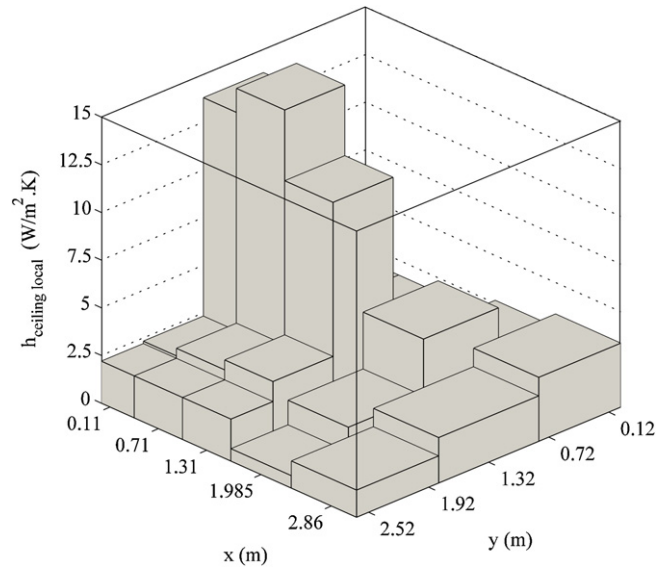


Fig. 5. Local CHTC at the ceiling calculated according to Eq. (6). $\Delta T_0 = 8.9 \text{ K}$ and 6.6 ACH, 2nd hour.

affected by the inlet flow. Moreover the inlet used for deriving the CHTC was smaller: 610 mm × 45 mm (width × height) at maximum, as against 830 mm × 80 mm in these experiments.

This comparison points out the specificity of existing correlations and the difficulty of extrapolating these models to similar cases. Inaccuracy in predicting the convective flow can occur when correlations are used outside of their range of application. Forced convective heat transfer is highly dependent on the inlet temperature and on the position, type and size of the inlet. Each configuration will lead to different correlations, due to the high gradient of velocity and temperature at the surface. Despite these difficulties, CHTC have to be defined accurately close to the inlet because a small error in the estimation of the CHTC might result in a large error in the room heat balance due to the high temperature gradients involved. Characterizing the flow at the ceiling at a smaller scale might be a solution to be able to generalize CHTC correlations.

4.2.3. Local values

In order to evaluate the accuracy of CHTC prediction using local velocity measurements, a mixed correlation has been developed based on these data (Eq. (6)). The mixed correlation is blending the natural convection term (correlation of Alamdari and Hammond for horizontal downward heat transfer [2]) and the forced convection term (correlation from ASHRAE for turbulent flow over a flat plate [1]), with a blending coefficient n equal to 6. The forced convective part is based on the local velocity measurements u_i .

$$Q_{\text{conv ceiling}} = \sum_{i=1}^{22} \left[\left(\frac{6.02 \cdot u_i^{0.8}}{D_h^{0.2}} \right)^n \left(\frac{\Delta T_{\text{Ceiling } i - \text{Inlet air}}}{\Delta T_{\text{Ceiling } i - \text{Room air}}} \right)^n + \left(0.6 \cdot \left(\frac{\Delta T_{\text{Ceiling } i - \text{Room air}}}{D_h^2} \right)^{1/5} \right)^n \right]^{1/n} \cdot \Delta T_{\text{Ceiling } i - \text{Room air}} \cdot A_i \quad (6)$$

of Fisher with the side-wall inlet [7], it can be observed that the measured CHTC are lower or equal to the proposed correlation. The correlation matches the experimental results only for 13 ACH because the jet is flowing over the entire surface in both cases; when the air change rate is lower, the jet is not attached to the ceiling anymore, resulting in a lower CHTC than the one obtained by Fisher. On the contrary, measured CHTC are usually larger than the correlation of Awbi and Hatton [6]. This can be explained by differences in the inlet configuration: in Awbi and Hatton's experiments, the inlet was located 50 cm inside the room, leading to an area not

An example of resulting convective heat transfer coefficients can be found in Fig. 5: a ratio 1–5 can be observed between the lowest CHTC and the highest one, close to the inlet. Fig. 6 compares the experimental data to the results obtained with the developed mixed correlation. The predicted convective heat transfer lies most of the time within the uncertainty bands. The highest inaccuracy in the developed equation can be observed for low inlet temperature, when the ceiling is much warmer than the room air. This is due to characteristics of the jet, which is falling down after the inlet and creating large variations in the local air temperature, whereas the developed equation is using a constant air temperature. When

Table 3

Comparison of the measured convective heat transfer over the 12 h of experiments with different CHTC correlations.

ACH (h^{-1})	3.3	6.7	6.8	6.6	13.1	13.2	13.1	13.3
ΔT_0 (K)	10.2	2.9	6.1	8.9	2.9	4.0	5.3	9.2
E_{exp} (Wh/m^2)	9.9	24.4	37.9	50.8	44.6	50.1	62.0	102.7
$\Delta E_{\text{Fisher-Exp}}$ (%)	900%	17%	74%	123%	-18%	-9%	0%	-1%
$\Delta E_{\text{Fisher and Pedersen-Exp}}$ (%)	1017%	77%	167%	241%	55%	74%	90%	89%
$\Delta E_{\text{Awbi and Hatton-Exp}}$ (%)	65%	-79%	-59%	-42%	-80%	-71%	-66%	-61%
$\Delta E_{\text{Eq.(6)-Exp}}$ (%)	93%	-15%	21%	35%	-21%	-13%	-9%	-11%

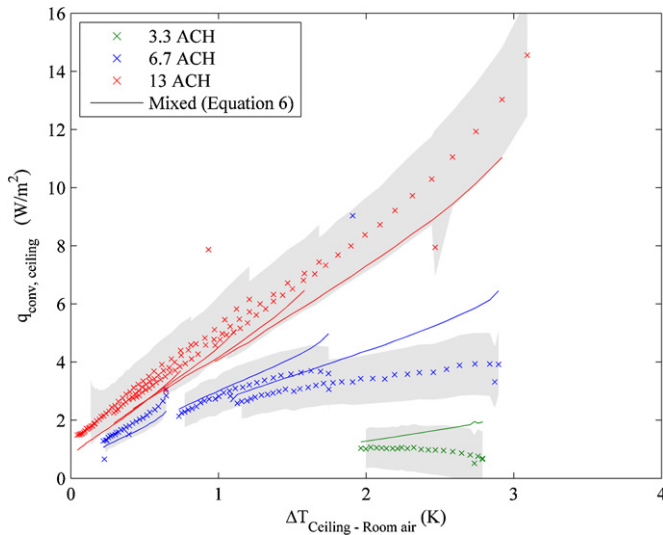


Fig. 6. Comparison of the experimental convective heat flux at the ceiling and the calculated values with Eq. (6).

comparing the calculated convective heat transfer with the different existing correlations (Table 3), it can be observed that the developed correlation gives better results than most of the correlations, with an average error of 17% (excluding 3.3 ACH).

4.3. CHTC at the walls

Fisher and Pedersen [8] proposed the following correlation for CHTC at the walls: $h = 0.19 \text{ ACH}^{0.8}$, using the inlet air as reference temperature. Experimental results are compared to this correlation

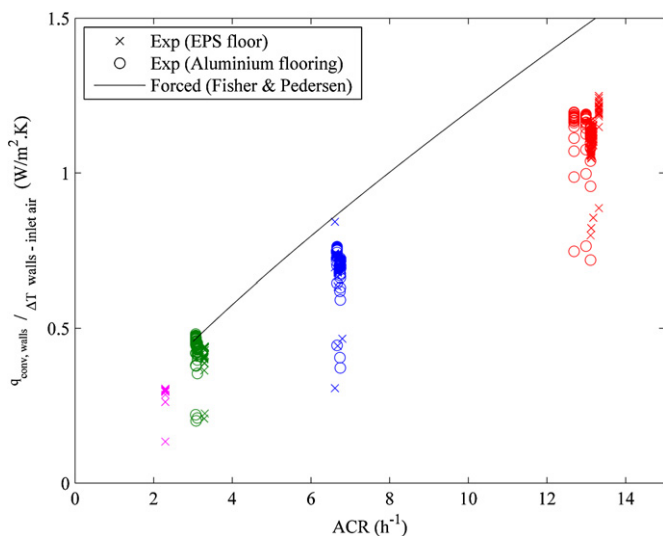


Fig. 7. CHTC at the walls depending on the air change rate. Mean uncertainty: (0.044 ACH) $\text{W/m}^2 \text{ K}$.

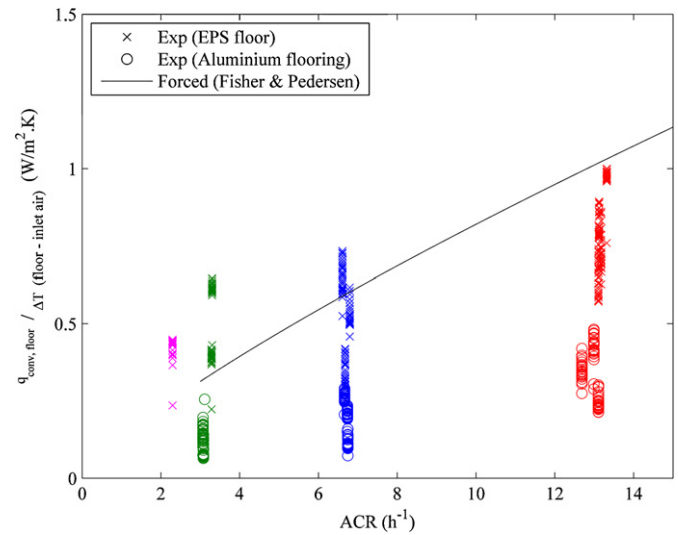


Fig. 8. CHTC at the floor depending on the air change rate. Mean uncertainty: (0.038 ACH) $\text{W/m}^2 \text{ K}$.

(Fig. 7), and it can be observed that Fisher and Pedersen's correlation overestimates the convective heat transfer for high air change rate.

4.4. CHTC at the floor

According to Fisher and Pedersen [8], the correlation for estimating CHTC at the floor is: $h = 0.13 \text{ ACH}^{0.8}$, using the inlet air as reference temperature. First it can be observed that experimental data for the floor made of EPS fit relatively well with the

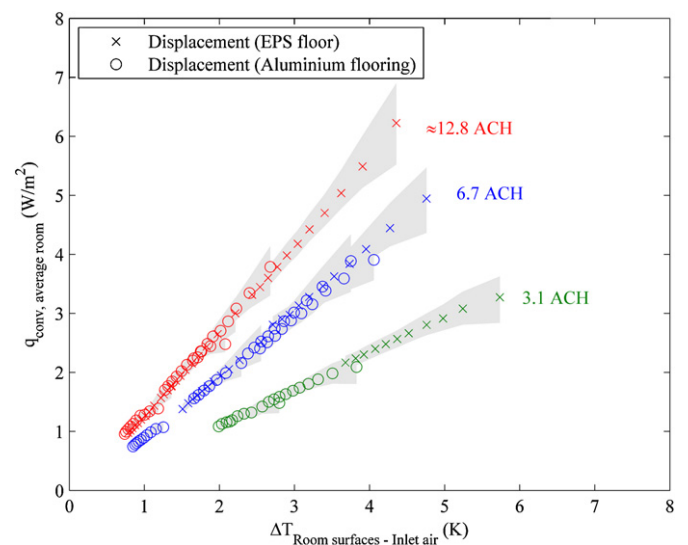


Fig. 9. Mean convective heat flux from all surfaces depending on the temperature difference between the mean surface temperature and the inlet air temperature – displacement ventilation.

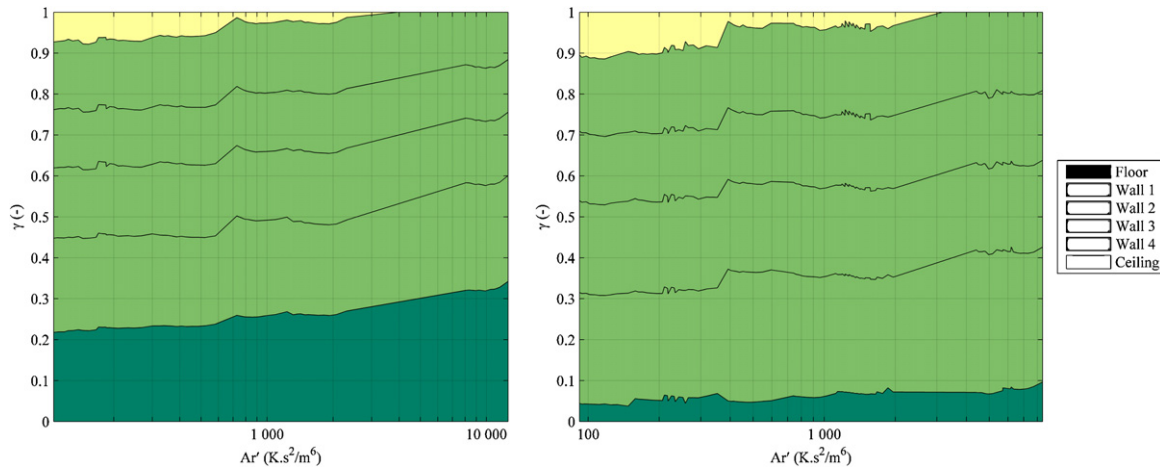


Fig. 10. Ratio of convective to total heat flow from the different surfaces depending on Ar' (left: floor made of EPS–right: aluminium flooring) – displacement ventilation.

correlation from Fisher and Pedersen, taking into consideration the uncertainty on the results (Fig. 8). But the CHTC at the floor is much lower with the aluminium flooring than with the floor made of EPS and does not fit with the correlation. In fact the temperature difference between the floor and the local air (30 mm far from the floor) is decreasing with the low-emissivity flooring. The ratio $\Delta T_{\text{Floor-Local air}}/\Delta T_0$ is decreasing by around 6% with the aluminium flooring. When using the inlet temperature as the reference temperature, the change in the local temperature profile is not taken into consideration, leading to an error in the prediction of the convective flux.

5. Results for displacement ventilation

5.1. Mean convective flow in the room and influence of the low-emissivity flooring

Fig. 9 presents the mean convective heat flux removed from the test room with displacement ventilation. It can be observed that this value remains the same with or without the aluminium flooring when the room thermal mass is located at the ceiling.

Fig. 10 shows the ratio of convective flux removed from each individual surface for displacement ventilation. Compared to mixing ventilation (Fig. 2), it can be observed that the convective flow from the ceiling is much smaller, most of the heat being removed on the other surfaces. Radiation plays therefore a major role in the room heat balance for displacement ventilation. Due to its low temperature, the convective flow extracted at the floor is rather high, removing at maximum one third of the heat. But when the floor is covered of an aluminium foil, the heat balance is modified, and the importance of the floor in the heat exchange is decreasing.

5.2. CHTC at the floor

Fig. 11 compares the experimental results to the correlation developed by Novoselac et al. [9]. They studied convective flow in a room equipped with displacement ventilation, supplying cold air between 3 and 10 ACH. The internal dimensions of the test room were 2.5 m × 3.9 m × 2.7 m (width × length × height) and the heat balance was performed dividing the room into 21 sections. The correlation for estimating the forced CHTC at the floor is: $h = 0.48 \text{ ACH}^{0.8}$, using the inlet air as reference temperature.

When the floor is made of EPS, there is a relatively good agreement between experimental results and the correlation. But when the floor is covered of an aluminium foil, the correlation from Novoselac et al. overestimates the convective flow from the floor.

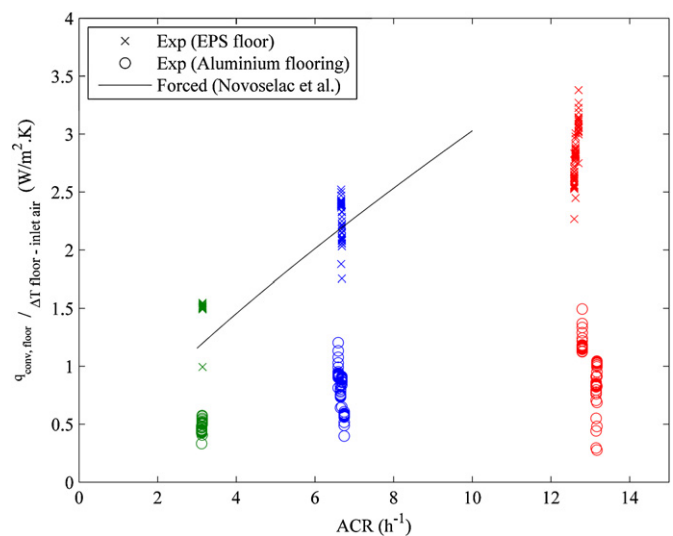


Fig. 11. CHTC at the floor depending on the air change rate. Mean uncertainty: $(0.123 \text{ ACH} + 0.64) \text{ W/m}^2 \text{ K}$.

This is due to the reference temperature used, as explained in part 4.4. For displacement ventilation, the ratio $\Delta T_{\text{Floor-Local air}}/\Delta T_0$ is decreasing by around 10% with the low-emissivity flooring.

5.3. CHTC at the other surfaces

For a room equipped with displacement ventilation, the convective flow observed at the walls and at the ceiling is natural, i.e. driven by buoyancy forces [9]. Therefore the CHTC at the ceiling is around 0.5 W/m^2 , and between 1 and 2 W/m^2 at the walls. Considering the uncertainty on the experimentally derived CHTC (which is around 1 W/m^2), it is therefore not possible to present results accurate enough for these surfaces.

6. Conclusion

In this work, a light room with a heavy ceiling was cooled down at constant air change rate and inlet temperature for a period of 12 h in order to simulate night-time ventilation. The results of the experiments conducted with a floor made of EPS were compared to the experiments with an aluminium flooring. Even though this change of emissivity did not influence the total convective flow removed from the test-room, some changes have been observed on

individual surfaces. The new flooring leads to a reorganization of the radiative and convective flow in the room: the radiative heat transfer, which previously occurred between the floor and the ceiling, is greatly reduced and reported to the walls. The efficiency of night-time ventilation should therefore not be affected by the presence of furniture, when the thermal mass is located at the ceiling.

Convective heat transfer coefficients (CHTC) have been derived from dynamic experiments and compared to existing correlations. The surface emissivity influences the value of forced CHTC due to the reference temperature used. It has also been observed that existing correlations give relatively accurate results for surfaces which are not directly affected by the inlet air, or for rooms equipped with displacement ventilation (Figs. 8 and 11). But the comparison also points out the specificity of existing correlations and the limitation of their range of application. Large deviations between models have been observed when modelling the forced convective heat transfer close to the inlet. High gradients in velocity and temperature make difficult to generalize values of CHTC for all types of inlet. One solution to overcome this problem could be to use local values of air velocity. This alternative way of deriving CHTC has been investigated theoretically by Alamdari and Hammond [20]; experimental results showed relatively accurate predictions (Fig. 6). CHTC could be estimated for different types of inlet, providing local velocity data from the flow theory. This will require a better integration of the flow characteristics in the building simulation programs, but the complexity of this task would be limited as the surface of interest is only the one directly affected by the inlet air, avoiding the complexity of dealing with recirculation. Another advantage of deriving local values of convective heat transfer is a better modelling of the radiative exchange and a more accurate evaluation of comfort.

References

- [1] ASHRAE, ASHRAE – Handbook Fundamentals – Chapter 4: Heat Transfer, American Society of Heating, Refrigeration and Air-Conditioning Engineers Inc., Atlanta, GA, 2009.
- [2] F. Alamdari, G.P. Hammond, Improved data correlations for buoyancy-driven convection in rooms, *Building Services Engineering Research and Technology* 4 (1983) 106–112.
- [3] H.B. Awbi, A. Hatton, Natural convection from heated room surfaces, *Energy and Buildings* 30 (1999) 233–244.
- [4] T. Min, L. Schutrum, G. Parmelee, J. Vouris, Natural convection and radiation in a panel-heated room, *ASHRAE Transactions* 62 (1956) 337–358.
- [5] A.J.N. Khalifa, R.H. Marshall, Validation of heat transfer coefficients on interior building surfaces using a real-sized indoor test cell, *International Journal of Heat and Mass Transfer* 33 (1990) 2219–2236.
- [6] H.B. Awbi, A. Hatton, Mixed convection from heated room surfaces, *Energy and Buildings* 32 (2000) 153–166.
- [7] D.E. Fisher, An Experimental Investigation of Mixed Convection Heat Transfer in a Rectangular Enclosure, Ph.D. thesis, University of Illinois at Urbana-Champaign, USA, 1995.
- [8] D. Fisher, C. Pedersen, Convective heat transfer in building energy and thermal load calculations, *ASHRAE Transactions* 103 (1997) 137–148.
- [9] A. Novoselac, B.J. Burley, J. Srebric, Development of new and validation of existing convection correlations for rooms with displacement ventilation systems, *Energy and Buildings* 38 (2006) 163–173.
- [10] I. Beausoleil-Morrison, Flow responsive modelling of internal surface convection, in: *Proceedings of Building Simulation' 01*, no. (1), International Building Performance Simulation Association, Rio de Janeiro, Brazil, 2001, pp. 923–930.
- [11] K. Goethals, H. Breesch, A. Janssens, Sensitivity analysis of predicted night cooling performance to internal convective heat transfer modelling, *Energy and Buildings* 43 (2011) 2429–2441.
- [12] EECAC (Energy Efficiency and Certification of Central Air Conditioners), Project for the Directorate General Transportation-Energy of the Commission of the European Union, Final Report, April 2003.
- [13] L. Pérez-Lombard, J. Ortiz, C. Pout, A review on buildings energy consumption information, *Energy and Buildings* 40 (2008) 394–398.
- [14] N. Artmann, H. Manz, P. Heiselberg, Climatic potential for passive cooling of buildings by night-time ventilation in Europe, *Applied Energy* 84 (2007) 187–201.
- [15] N. Artmann, D. Gyalistras, H. Manz, P. Heiselberg, Impact of climate warming on passive night cooling potential, *Building Research and Information* 36 (2008) 111–128.
- [16] J.M. Salmeron, J.A. Sanz, F.J. Sanchez, S. Alvarez, A. Pardo, Flow pattern effects on night cooling ventilation, *International Journal of Ventilation* 6 (1) (2007) 21–30.
- [17] N. Artmann, R.L. Jensen, H. Manz, P. Heiselberg, Experimental investigation of heat transfer during night-time ventilation, *Energy and Buildings* 42 (2010) 366–374.
- [18] P. Wallenten, Convective heat transfer coefficients in a full-scale room with and without furniture, *Building and Environment* 36 (2001) 743–751.
- [19] K. Goethals, M. Delghust, G. Flamant, M. De Paepe, A. Janssens, Experimental investigation of the impact of room/system design on mixed convection heat transfer, *Energy and Buildings* 49 (2012) 542–551.
- [20] F. Alamdari, G.P. Hammond, Time-dependent convective heat transfer in warm-air heated rooms, in: *Proc. Int. Symp. Energy Conservation in the Built Environment*, vol. 4, CIB/An Foras Forbartha, Dublin, 1987, pp. 209–220.
- [21] W. Kessling, S. Holst, M. Schuler, Innovative design concept for the New Bangkok International Airport, NBIA, in: *Symposium on Improving Building Systems in Hot and Humid Climates*, Dallas, 2004.
- [22] CEN, International Standard ISO 13786:2007, Thermal Performance of Building Components – Dynamic Thermal Characteristics – Calculation Methods, 2007.
- [23] J. Le Dréau, L. Karlén, M. Litewnicki, L. Michaelsen, A. Møllerskov, H. Odegaard, L. Svendsen, R.L. Jensen, A. Marszal, Experimental investigation of the influence of different flooring emissivity on night-time cooling using displacement ventilation, in: *Proceedings of the 9th Nordic Symposium on Building Physics NSB 2011*, Tampere University Press, 2011, pp. 491–498.
- [24] R.L. Jensen, O. Daniels, R.O. Justesen, M.S. Madsen, K.B. Mikkelsen, J. Nørgaard, C. Topp, Experimental investigation of the heat transfer in a room using night-time cooling by mixing ventilation, in: *Proceedings of the 9th Nordic Symposium on Building Physics NSB 2011*, Tampere University Press, 2011, pp. 507–516.
- [25] G.D. Smith, *Numerical Solution of Partial Differential Equations*, Oxford University Press, New York, 1965.
- [26] J.R. Ehlert, T.F. Smith, View factors for perpendicular and parallel rectangular plates, *Journal of Thermophysics and Heat Transfer* 7 (1) (1993) 173–174.
- [27] CIBSE Guide A3, Thermal Properties of Buildings and Components, Chartered Institution of Building Services Engineers, London, UK, 1999.
- [28] J. Crabol, *Transfert de Chaleur: Applications Industrielles*, Tome 2, Masson, Paris, 1990.
- [29] J. Clarke, 7 – Energy-related subsystems, in: *Energy Simulation in Building Design*, second ed., Butterworth-Heinemann, Oxford, 2001, pp. 202–280.
- [30] A.J. Chapman, *Fundamentals of Heat Transfer*, fourth ed., New York, McMillan, 1984.
- [31] S.W. Churchill, R. Usagi, A general expression for the correlation of rates of transfer and other phenomena, *AIChE Journal* 18 (1972) 1121–1128.
- [32] I. Beausoleil-Morrison, The Adaptive Coupling of Heat and Air Flow Modelling within Dynamic Whole-Building Simulation, Ph.D thesis, University of Strathclyde, Glasgow, 2000.
- [33] A. Novoselac, B.J. Burley, J. Srebric, New convection correlations for cooled ceiling panels in room with mixed and stratified airflow, *HVAC&R Research* 12 (2006) 279–294.
- [34] L. Neiswanger, G.A. Johnson, V.P. Carey, An experimental study of high Rayleigh number mixed convection in a rectangular enclosure with restricted inlet and outlet openings, *Journal of Heat Transfer* 109 (1987) 446–453.
- [35] L. Peeters, I. Beausoleil-Morrison, A. Novoselac, Internal convective heat transfer modelling: critical review and discussion of experimentally derived correlations, *Energy and Buildings* 43 (2011) 2227–2239.
- [36] N. Artmann, R. Vonbank, R.L. Jensen, Temperature Measurements using Type K Thermocouples and the Fluke Helios Plus 2287A data logger, Internal Report, Aalborg University, [http://vbn.aau.dk/en/publications/temperature-measurements-using-type-k-thermocouples-and-the-fluke-helios-plus-2287a-datalogger\(1d86f910-bbc1-11dd-887e-000ea68e967b\).html](http://vbn.aau.dk/en/publications/temperature-measurements-using-type-k-thermocouples-and-the-fluke-helios-plus-2287a-datalogger(1d86f910-bbc1-11dd-887e-000ea68e967b).html) (2008).
- [37] N. Artmann, R.L. Jensen, Night-time Ventilation Experiments – Setup, Data Evaluation and Uncertainty Assessment, Internal Report, Aalborg University, [http://vbn.aau.dk/en/publications/nighttime-ventilation-experiments\(9691ccd0-bbc2-11dd-887e-000ea68e967b\).html](http://vbn.aau.dk/en/publications/nighttime-ventilation-experiments(9691ccd0-bbc2-11dd-887e-000ea68e967b).html), 2008.